



CHORUS

This is the accepted manuscript made available via CHORUS. The article has been published as:

Lattice instability during phase transformations under multiaxial stress: Modified transformation work criterion

Valery I. Levitas, Hao Chen, and Liming Xiong

Phys. Rev. B **96**, 054118 — Published 29 August 2017

DOI: [10.1103/PhysRevB.96.054118](https://doi.org/10.1103/PhysRevB.96.054118)

Lattice instability during phase transformations under multiaxial stress: modified transformation work criterion

Valery I. Levitas^{1,2}, Hao Chen³, Liming Xiong³

¹*Iowa State University, Departments of Aerospace Engineering, Mechanical Engineering, and Material Science and Engineering, Ames, Iowa 50011, USA*

²*Ames Laboratory, Division of Materials Science and Engineering, Ames, IA, USA*

³*Iowa State University, Department of Aerospace Engineering, Ames, Iowa 50011, USA*

A conceptually novel continuum/atomistic approach for predicting lattice instability during crystal-crystal phase transformations (PTs) is developed for the general loading with an arbitrary stress tensor and large strains. It is based on the synergistic combination of the generalized Landau-type theory for PTs and molecular dynamics (MD) simulations. The continuum approach describes the entire dissipative transformation process in terms of an order parameter, and the general form of the instability criterion is derived utilizing the second law of thermodynamics. The feedback from MD allowed us to present the instability criterion for both direct and reverse PTs in terms of the critical value of the modified transformation work, which is linear in components of the true stress tensor. It was calibrated by MD simulations for direct and reverse PTs between semiconducting silicon Si I and metallic Si II phases under just two different stress states. Then, it describes hundreds of MD simulations under various combinations of three normal and three shear stresses. In particular, the atomistic simulations show that the effects of all three shear stresses along cubic axes on lattice instability of Si I are negligible, which is in agreement with our criterion.

Keywords: Triaxial stress states; Phase Transformation; Lattice Instability; Phase field; Molecular dynamics

I. INTRODUCTION

Instability of the crystal lattice under nonhydrostatic loading is a key process for understanding and quantitative studies of various phenomena, including PTs between two crystalline phases, melting, amorphization, fracture, twinning, and dislocation nucleation. The traditional approach [1, 2, 3, 4, 5, 6, 7, 8, 9, 10, 11, 12] (coined as the generalized Born criterion) states

that lattice instability occurs when $\det \mathbf{C} = 0$ for the first time, where \mathbf{C} are the generalized elastic moduli. This general condition for different symmetries of the deformed lattice transforms to conditions that some elastic moduli or their combinations reduce to zero, which results in various reasonable/successful applications. For multilattices, relative shift vectors are included in instability criteria along with elastic moduli within the same description [9, 13, 11, 12]. In addition, phonon stability (soft-mode) criteria [9, 13, 7, 8, 11, 12] were applied. However,

(a) There are many cases when instability is not related to any of these criteria. For direct and reverse PTs between semiconducting Si I and metallic Si II phases, see [14] and the MD simulations below. For many other materials, while some softening is observed, elastic moduli and phonon frequencies are still far from 0 [11, 12, 14, 15, 16].

(b) There are also fundamental problems with the generalized Born approach. All of the above instabilities are related to inelastic structural changes, which generate dissipation and require order parameters for their description, which were neglected in [9, 2, 3, 4, 5, 7, 8, 11, 12, 13, 14, 15].

(c) Instability criteria describe not only material properties but also include loading conditions (device). They are different for different prescribed stresses, e.g., true Cauchy stress $\boldsymbol{\sigma}$ (force per unit actual area) or first Piola-Kirchhoff stress \mathbf{P} (force per unit undeformed area). Results are also different for different choice of the finite strains measures [2, 3, 4], which is practically arbitrary. In simulations of heterogeneous microstructure evolution in materials under mechanical loadings, stress components can be prescribed at boundary only and it is impossible to define, which of the stress tensors is controlled in each material point within bulk material. Consequently, such instability criteria cannot be directly applied in continuum simulations.

(d) Elastic moduli and phonon spectra should be calculated directly in atomistic simulations for each multiaxial strain state and it is practically impossible to develop a predictive analytical theory determining which combination of six components of $\boldsymbol{\sigma}$ leads to initiation of a PT.

Here, we developed a conceptually novel approach to predict lattice instability during crystal-crystal PTs by combining generalized Landau-type theory for PTs and MD simulations for direct and reverse PTs between Si I and Si II phases.

(a) The continuum approach includes an order parameter η describing the entire transfor-

mation process (like in Landau-type theory for PTs) and the general form of the instability criterion is strictly derived utilizing the second law of thermodynamics.

(b) This criterion is independent of the prescribed stress tensor measure, which is confirmed by MD simulations.

(c) The feedback from MD allowed us to present the instability criterion for both direct and reverse PTs in terms of the critical value of the modified transformation work; the criterion is calibrated by MD simulations for Si at two different stress states; then the criterion describes hundreds of MD simulations under various combinations of triaxial normal stresses and shear stresses.

(d) The effect of all three shear stresses along cubic axes on the lattice instability of Si I was negligible in atomistic simulations, in agreement with the simplest version of our criterion.

(e) The effect of the jumps in elastic moduli during PT on the instability criterion is negligible, which drastically simplifies both the instability criterion and the Landau-type theory.

(f) Good correspondence between theory and simulations is obtained only for the case when local theory takes into account a geometrically nonlinear term contributing to interfacial stresses for general heterogeneous solutions, which was traditionally neglected in the Landau-type theory. This, however, does not mean that interfaces or interface stresses affect our criterion, because it is formulated for homogeneous states.

(g) For PT Si I \rightarrow Si II, instability also corresponds to the generalized Born criterion when the Cauchy stress is prescribed, i.e., known results when one of the traditional criteria is predictive may be consistent with our criterion as well. However, for the reverse PT, Si II \rightarrow Si I, the traditional approach is not applicable while our criterion still holds.

(h) Comparison of theoretical and MD results mentioned in (c)-(g) leads to a significant advancement of the generalized Landau theory, in particular, in terms of unexpected dependence of transformation strain and free energy on the order parameter and elastic strain.

Tensors are designated with boldface symbols; contractions of tensors $\mathbf{A} = \{A_{ij}\}$ and $\mathbf{B} = \{B_{ji}\}$ are designated as $\mathbf{A}\cdot\mathbf{B} = \{A_{ij} B_{jk}\}$ and $\mathbf{A}:\mathbf{B} = A_{ij} B_{ji}$; \mathbf{I} is the unit tensor; and the transpose of \mathbf{A} is \mathbf{A}^T .

II. LATTICE INSTABILITY CRITERION

Similar to the previous works [2, 3, 4, 5, 7, 8, 9, 11, 12, 13] and thermodynamic textbooks, we are looking for instability criterion for homogeneously stressed material under homogeneous infinitesimal fluctuations, i.e., instability of the local constitutive equations. After this criterion is satisfied, material transforms to the alternative phase either homogeneously or, if heterogeneous perturbations are present (due to thermal fluctuation or numerical errors in continuum approaches), heterogeneously, see Figs. 1, 2, and 3, and supplemental movies [17]. However, transformation process that occurs after instability criterion is met does not affect the criterion itself, i.e., the instability criterion does not contain information about any heterogeneities and interfaces.

Let $\mathbf{U}_t = \mathbf{I} + \bar{\boldsymbol{\varepsilon}}_t$ be the symmetric transformation deformation gradient that transforms the crystal lattice of the parent phase 1 into the crystal lattice of the product phase 2 when both are under stress-free conditions. We decompose $\bar{\boldsymbol{\varepsilon}}_t$ into spherical ε_{0t} and deviatoric \mathbf{e}_t parts, $\bar{\boldsymbol{\varepsilon}}_t = 1/3\varepsilon_{0t}\mathbf{I} + \mathbf{e}_t$. Note that (excluding small strains) ε_{0t} is not a volumetric strain, so \mathbf{e}_t is not just change in shape. The order parameter η encodes the transformation process: for (meta)stable phases $\eta = \hat{\eta}$, where $\hat{\eta} = 0$ for phase 1 or $\hat{\eta} = 1$ for phase 2. The multiplicative decomposition of the deformation gradient $\mathbf{F} = \mathbf{F}_e \cdot \mathbf{U}_t$ into elastic \mathbf{F}_e and transformational \mathbf{U}_t contributions will be used. The Landau-type theory for PTs under large strains, which includes formulation of lattice instability conditions under spontaneous variations of the order parameters, was developed in [18] but without allowing for interfacial stresses. Generalization for the case with interfacial stresses was completed in [19] but without the consideration of the instability conditions. Here we will generalize the instability criteria in [18] for the case with interfacial stresses, see Appendix. We demonstrate that despite the fact that we consider homogeneous states here, modification in the local Helmholtz energy per unit initial volume ψ required for allowing the interface stresses is important for a formulation of the final instability criterion. Then, we specify and validate these criteria utilizing MD simulations.

A. General expression

Using the thermodynamics laws, the dissipation rate due to PT [18] can be derived as

$$D = X\dot{\eta} \geq 0; \quad X := \mathbf{P}^T \cdot \mathbf{F}_e : \frac{\partial \mathbf{U}_t(\eta)}{\partial \eta} - \frac{\partial \psi(\mathbf{E}_e, \theta, \eta)}{\partial \eta}, \quad (1)$$

where X is the thermodynamic force for change in η , $\mathbf{E}_e = 0.5(\mathbf{F}_e^T \cdot \mathbf{F}_e - \mathbf{I})$ is the Lagrangian elastic strain, and θ is the temperature. Determination of η -dependence of \mathbf{U}_t and ψ is one of the main problems in formulation of the Landau-type theories. These dependences should satisfy the constraint that $X = 0$ for $\eta = \hat{\eta}$ for any stress \mathbf{P} , temperature θ , and elastic deformation gradient \mathbf{F}_e ; otherwise, equilibrium phases will not correspond to $\eta = \hat{\eta}$, see Appendix. The following thermodynamic definition of the lattice instability under prescribed (constant) stress \mathbf{P} and temperature is suggested:

if a spontaneous deviation of the order parameter $\Delta\eta$ from the thermodynamic equilibrium values $\hat{\eta}$ is thermodynamically admissible, i.e., dissipation rate $D \geq 0$, then the thermodynamic equilibrium is unstable.

Such a definition results in the following general form of the instability condition (see Appendix):

$$\frac{\partial X(\mathbf{P}, \mathbf{F}_e, \hat{\eta})}{\partial \eta} = \mathbf{P}^T \cdot \mathbf{F}_e \cdot \frac{\partial^2 \mathbf{U}_t(\hat{\eta})}{\partial \eta^2} - \frac{\partial^2 \psi(\mathbf{E}_e, \hat{\eta})}{\partial \eta^2} \geq 0, \quad (2)$$

where $\hat{\eta} = 0$ corresponds to criterion for $1 \rightarrow 2$ PT and $\hat{\eta} = 1$ is for criterion for $2 \rightarrow 1$ PT. Note that perturbations in \mathbf{F}_e were also taken into account but they do not contribute to the final expression. It is proven Appendix that *the PT criterion (2) is valid independent of the change of the prescribed stress measure*; in particular, it is valid for the prescribed Cauchy stress.

While formally correct, the PT criterion (2) does not have any predictive capability and was never applied to any material even for uniaxial loading due to the following reasons: it requires knowledge of the energy and nonlinear elasticity rule vs. \mathbf{E}_e and also vs. η as well as \mathbf{U}_t versus η , which were not determined for any material. Even definition and physical meaning of the order parameter is not clear; in most applications this is just some internal variable. It is much more difficult to determine even just $\psi(\mathbf{E}_e)$ than the elastic moduli \mathbf{C} , required for the generalized Born criterion. Below, we synergistically combine Eq.(2) and MD simulation and obtain simple predictive lattice instability criterion (12) and significant advancement/specification of the Landau-type theory for PTs, both under all six components of stress tensor.

The variable transformation deformation gradient that describes the transformation process

1 \leftrightarrow 2 is $\mathbf{U}_t(\eta) = \mathbf{I} + \boldsymbol{\varepsilon}_t(\eta)$ with

$$\boldsymbol{\varepsilon}_t(\eta) = 1/3\varepsilon_{0t}\varphi(a_1, \eta)\mathbf{I} + \mathbf{e}_t\varphi(a_2, \eta); \quad \varphi(a, \eta) := a\eta^2(1 - \eta)^2 + (4\eta^3 - 3\eta^4), \quad (3)$$

where a_i are the material parameters. Traditionally (see [18, 19] and references), $a_1 = a_2$ and all components of transformation strain change proportionally during PT, which was a strong assumption. To describe MD results, we need to use *different parameters for spherical and deviatoric transformation strain*. The Helmholtz free energy for homogeneous states is accepted as [19]:

$$\psi(\mathbf{E}_e, \eta, \theta) = \psi^e(\mathbf{F}_e, \eta, \theta) + J\check{\psi}^\theta(\theta, \eta) + \tilde{\psi}^\theta(\theta, \eta); \quad J = \det\mathbf{F}. \quad (4)$$

$$\check{\psi}^\theta = A(\theta)\eta^2(1 - \eta)^2; \quad \tilde{\psi}^\theta = \Delta G^\theta(\theta)\eta^3(4 - 3\eta). \quad (5)$$

Here, ψ^e is the elastic energy; $\check{\psi}^\theta$ is the double-well barrier; $\tilde{\psi}^\theta$ is the part of the thermal energy proportional to the difference between the thermal parts of the energies of phases 2 and 1, ΔG^θ . It is justified in [19] that for correct introduction of the interfacial stresses in the Ginzburg-Landau theory for an interface between two phases, along with modifications in the gradient energy, the local double-well barrier $\check{\psi}^\theta$ should be also multiplied by J . Thus, while we consider homogeneous states and interfaces are not present, still we have the term J , which is required for consistent interfacial stresses for heterogeneous states. This should not be surprising, because for two phase states $\check{\psi}^\theta$ is localized at the interfaces, i.e., where $0 < \eta < 1$, and is zero in the bulk, where $\eta = 0$ or 1 . While for homogeneous stable states $\eta = 0$ or 1 and $\check{\psi}^\theta = 0$, the second derivative of $\check{\psi}^\theta$ at $\eta = 0$ or 1 is not zero, which makes contribution to the instability conditions. Substituting Eqs.(3) and (4) and $\mathbf{P} = J\boldsymbol{\sigma}\cdot\mathbf{F}^{T-1}$ in Eq.(2), we obtain

$$W := \boldsymbol{\sigma}\cdot\mathbf{F}_e^{T-1} \cdot \mathbf{U}_t^{-1} \cdot \frac{\partial^2\mathbf{U}_t}{\partial\eta^2} \cdot \mathbf{F}_e^T \geq \frac{1}{J} \frac{\partial^2\psi^e}{\partial\eta^2} + \frac{\partial^2\check{\psi}^\theta}{\partial\eta^2} + \frac{1}{J} \frac{\partial^2\tilde{\psi}^\theta}{\partial\eta^2}; \quad \eta = \hat{\eta}. \quad (6)$$

B. Specifications

The first term in the right-hand side is due to variation of elastic parameters of i^{th} order $\mathbf{C}^i(\eta)$, $i = 2, 3, \dots$, during PT, which produces nonlinear contributions in strain \mathbf{E}_e , and consequently, stresses. MD simulations below demonstrate that instability criterion is linear in

stresses, i.e., contribution of this term should be negligible. This term can be eliminated if $d^2\mathbf{C}^i(\hat{\eta})/d\eta^2 = 0$, e.g., for

$$\mathbf{C}^i(\eta) = \mathbf{C}_1^i + (\mathbf{C}_2^i - \mathbf{C}_1^i)\chi(\eta) \quad \text{with} \quad \chi(\eta) := \eta^3(10 - 15\eta + 6\eta^2). \quad (7)$$

This gives a general idea for formulating the Landau potential: different interpolation functions can be used for different material properties, and if some properties should not contribute to instability conditions, function $\chi(\eta)$ can be used. For PT $1 \rightarrow 2$, i.e., for $\eta = 0$, $\mathbf{U}_t = \mathbf{I}$, direct calculations show that the last term also disappears, and Eq.(6) simplifies to

$$W = \boldsymbol{\sigma}:\mathbf{F}_e^{T-1} \cdot \frac{\partial^2 \mathbf{U}_t(0)}{\partial \eta^2} \cdot \mathbf{F}_e^T \geq 2A(\theta). \quad (8)$$

Eq.(8) is our final instability criterion for general loading.

The general form of the Cauchy stress is

$$\boldsymbol{\sigma} = \begin{bmatrix} \sigma_{11} & \tau_{12} & \tau_{13} \\ \tau_{12} & \sigma_{22} & \tau_{23} \\ \tau_{13} & \tau_{23} & \sigma_{33} \end{bmatrix}. \quad (9)$$

The formulas for the total and elastic deformation gradients are

$$\mathbf{F} = \begin{bmatrix} F_{11} & F_{12} & F_{13} \\ 0 & F_{22} & F_{23} \\ 0 & 0 & F_{33} \end{bmatrix}, \quad \mathbf{F}_e = \begin{bmatrix} F_{11}^e & F_{12}^e & F_{13}^e \\ 0 & F_{22}^e & F_{23}^e \\ 0 & 0 & F_{33}^e \end{bmatrix}, \quad (10)$$

where zeros under the diagonal are due to our way of excluding the rigid-body rotation. We will focus on the cubic to tetragonal transformation considered in MD simulations below, for which normal transformation strains are $\varepsilon_{t1} = \varepsilon_{t2}$ and ε_{t3} , and off-diagonal components are zero. In Eq.(11) we consider slightly more general case $\varepsilon_{t1} \neq \varepsilon_{t2}$, like for cubic to monoclinic PT without transformation shears. Substituting Eqs.(9) and (10) into Eq.(8), one obtains the explicit expression for W for this case:

$$W = a_1\sigma_0\varepsilon_{0t} + a_2\mathbf{S}:\mathbf{e}_t + a_2[\tau_{13}F_{13}^e(e_{t3} - e_{t1})/F_{33}^e + \tau_{23}F_{23}^e(e_{t3} - e_{t2})/F_{33}^e + \tau_{12}F_{12}^e(e_{t2} - e_{t1})/F_{22}^e + \tau_{13}F_{12}^eF_{23}^e(e_{t1} - e_{t2})/(F_{22}^eF_{33}^e)]. \quad (11)$$

where $\sigma_0 := 1/3\boldsymbol{\sigma}:\mathbf{I}$ is the mean stress and \mathbf{S} is the deviatoric stress. While off-diagonal components of the transformation deformation gradient are zero, shear stresses still contribute to the modified transformation work. Since the terms proportional to the shear stresses are quadratic or cubic in components of the elastic and transformational deformation gradients, they disappear in the geometrically linear approximation.

For the particular case of loading by three stresses normal to the cubic faces, all tensors in Eq.(8) are coaxial, \mathbf{F}_e^{T-1} and \mathbf{F}_e^T eliminate each other, all terms with shear stresses in Eq.(11) disappear, and we obtain the following instability criterion:

$$W = a_1\sigma_0\varepsilon_{0t} + a_2\mathbf{S}:\mathbf{e}_t \geq A(\theta). \quad (12)$$

Since W represents a modified transformation work (for $a_1 = a_2 = 1$ it transforms to the transformation work), the criterion (12) (and the general criterion (8)) will be called the critical modified transformation work criterion. Similar criterion can be obtained for the reverse PT $2 \rightarrow 1$ by placing $\eta = 1$. This was done, but results will be presented for the case when phase 2 was considered as the reference phase and the same criteria (8) and (12) are applicable with \mathbf{U}_t^{-1} instead of \mathbf{U}_t .

III. SIMULATION METHOD

In this work, classical MD simulations were performed using the LAMMPS package [20]. The employed interatomic force field for the interactions between Si atoms was from the Tersoff interatomic potential [21]. This potential has been demonstrated to be successful in describing the crystal structure transition from the diamond-cubic to β -Sn in single crystal silicon (Si I to Si II) under a uniaxial stress of ~ 12 GPa (see [22] and current results), which is close to the experimental value [23]. Advantage of the the Tersoff interatomic potential for the description of Si I to Si II PT in comparison with four other potentials is demonstrated in [24]. The majority of simulations have been performed for a Si sample containing 64,000 atoms. To prove a size-independence of the results, simulations under uniaxial loading were performed for varying sample sizes of 5nm to 40nm, which contained 8,000 to 4,096,000 atoms. A time step of 1 fs was used in all simulations. The system temperature is set as $\theta = 1K$ to eliminate the possibility of the occurrence of thermally activated PTs. Effects of the free surfaces on the PTs were excluded by employing periodic boundary conditions along all three cubic directions, except the direction along which the first Piola-Kirchhoff stress was applied. For uniaxial loading, simulations were conducted under (a) a specified first Pila-Kirchhoff stress; (b) a specified Cauchy stress; and (c) a strain-controlled loading. Here the first Piola-Kirchhoff stress was applied to the system by enforcing constant forces on the top and bottom layers of

the atomistic system along the directions of compression. The Cauchy stress was applied to the system using the Berendsen algorithm [25], in which the instantaneous stress of the system was calculated using the virial formula and controlled in two steps. First, a Cauchy stress increment of 0.01 GPa was applied to the simulation cell; this was then followed by an equilibration of the entire specimen for 10 ps. In order to ensure that a desired Cauchy stress has been achieved, the system virial stress at the end of each loading increment was calculated and was checked against the prescribed stress, assuming that the averaged Cauchy stress coincides with the virial stress [26]. It should be noted that such a weak-coupling stress-controlling strategy is different from that of using the Parinello-Rahman algorithm [27], which, in contrast, approximately controls the deviatoric component of the second Piola-Kirchhoff stress [28]. In the strain-controlled loading, the fix deform method in LAMMPS was employed. That is, each time after the simulation box size along the main loading direction was changed at a value of 0.2 angstrom, the system was equilibrated for 100 ps. This equilibration process occurred with a fixed box size along the loading direction and zero stress along the other direction. Multiaxial loading was performed under controlled normal components of the Cauchy stress utilizing the Berendsen algorithm [25]. However, shear stresses in LAMMPS cannot be applied with the Berendsen algorithm. They were applied with the Parinello-Rahman algorithm [27], which controls the deviatoric part of the second Piola-Kirchhoff stress [28].

The instability point was determined by the largest applied Cauchy stress σ_3 for PT Si I \rightarrow Si II and by the smallest applied Cauchy stress σ_3 for PT Si II \rightarrow Si I that can be equilibrated. The Cauchy stress at the instability points were substituted into the instability criteria. Beyond the instability points, the system evolves fast to the alternative phase at the fixed Cauchy stress, which is not of interest. To reproduce an equilibrium unstable branch of the stress-strain curves in Fig. 3b, we used the strain-controlled loading which requires relatively long computations. To approximately find the quasi-equilibrium unstable branch of the stress-strain curves in Fig. 3 we used the Berendsen method with the damping parameter of 1 ps (which corresponds to 1000 time steps) and the fictitious "bulk modulus" of 100 GPa, which were determined by experimenting. The difference between the two approaches is very small.

IV. SIMULATION RESULTS AND DISCUSSION

In order to formulate and confirm the lattice instability criterion (12), MD results for cubic-tetragonal PTs Si I \leftrightarrow Si II have been first obtained for various combinations of three normal prescribed Cauchy stresses σ_i along cubic axes (100); negative stresses are compressive, and compressive σ_3 has the largest magnitude.

Components $\varepsilon_{t1} = \varepsilon_{t2} = 0.1753$ and $\varepsilon_{t3} = -0.447$, therefore, $\varepsilon_{t0} = -0.0964$ have been determined by comparing crystal lattice of Si I and II at zero stresses. Note that $\varepsilon_{t0} = -0.0964$ is much smaller in the magnitude than volumetric strain $J - 1 = -0.236$. Then for the reverse PT $\mathbf{U}_t^r = \mathbf{U}_t^{-1}$, i.e., components $\varepsilon_{t1}^r = \varepsilon_{t2}^r = -0.1492$, $\varepsilon_{t3}^r = 0.8083$, and therefore $\varepsilon_{t0} = 0.5099$ (which is much larger than the volumetric strain $1/J - 1 = 0.3089$).

A. Transformation process

A typical phase transformation processes, which was found in our MD simulations, is presented in Figs. 1 and 2 and supplementary movies [17]. They are visualized using OVITO [29], with colors representing the local von-Mises shear strain, calculated as described in [30, 31]. The stress-free state of Si I was utilized as the reference state. The cutoff used in OVITO is 2.8Å for all shear strains in the paper. The same two-phase structure was found while the cutoff was varied from 2.4Å to 3Å. First, due to fluctuation of the stress, nucleation of the product phase occurs. Then nuclei grow, form the bands which fill the entire sample.

B. Stress-strain curves

Typical uniaxial stress - strain curves for $\boldsymbol{\sigma}$, \mathbf{P} , and the second Piola-Kirchhoff stress $\mathbf{T} = \mathbf{F}^{-1} \cdot \mathbf{P}$ for direct and reverse PTs are shown in Fig. 3 under prescribed $\boldsymbol{\sigma}$, \mathbf{P} , and displacements (strains). For prescribed $\boldsymbol{\sigma}$, instability for PT Si I \rightarrow Si II starts at maximum Cauchy stress (point I , $E = 0.2293$), i.e., at zero value of corresponding elastic modulus, which is typical here for multiaxial loading as well; \mathbf{P} and \mathbf{T} continue growing beyond the instability point I . However, reverse PT starts at a minimum stress but *nonzero value of any elastic moduli*, i.e., it cannot be described by traditional generalized Born approach. Instability is easily detected by the impossibility of equilibrating the system under fixed $\boldsymbol{\sigma}$ until it transforms to an alternative phase. After instability point I , the microstructure initially evolves homogeneously, then heterogeneously with stochastic fluctuations, then with bands consisting of some intermediate phases (Fig. 3). At larger strains, bands with fully formed Si II appear and grow. However, if

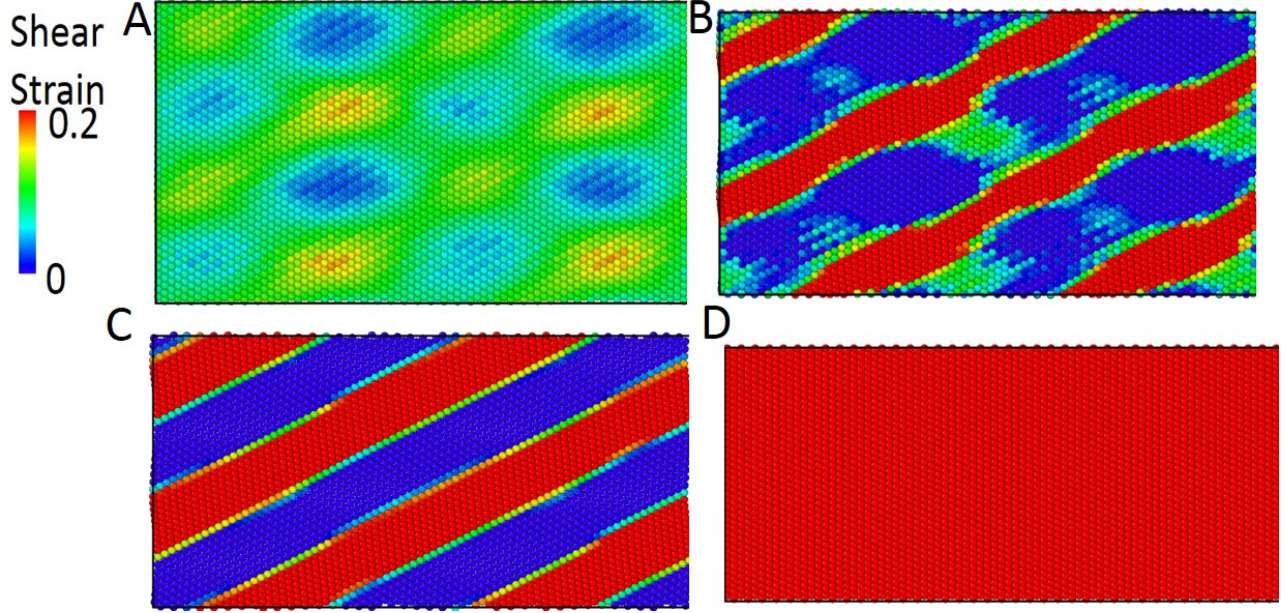


Figure 1: Phase transformation process for Si I→Si II under uniaxial loading. (A) heterogeneous nucleation of Si II due to stress fluctuation. (B) and (C) due to internal stresses caused by the transformation strain, complete Si II and residual Si I reshape into bands. Note that Si I bands are formed through the reverse PT. (D) Final stable state of Si II.

starting with band structure, the stress increases (i.e., strain reduces) toward instability point I , heterogeneous fluctuating structure is observed even in the vicinity of instability point I (Fig. 3). Thus, multiple solutions—including homogeneous and various heterogeneous ones—are observed after instability. Importantly, instability under heterogeneous perturbations does not start earlier than it is determined by criterion (12) under homogenous perturbations. This is consistent with the Ginzburg-Landau theory, because any heterogeneity is penalized by the gradient energy. Thus, theory for homogeneous fluctuations is sufficient for the prediction of lattice instability.

When the first Piola-Kirchhoff stress \mathbf{P} was prescribed instead of $\boldsymbol{\sigma}$, the *stress-strain curves and instability point I did not change*. This is in agreement with predictions of our approach and in contrast to the generalized Born approach [2, 3, 4, 5, 7, 8]. Since \mathbf{P} continues growing after instability for some stress increment until $E = 0.2610$, the sample with homogeneous microstructure still can be equilibrated until maximum of \mathbf{P} . In the Ginzburg-Landau simulations this solution would correspond to nonzero η , i.e., some intermediate homogenous phase. Since in MD we cannot distinguish elastic and transformation strains for the intermediate states,

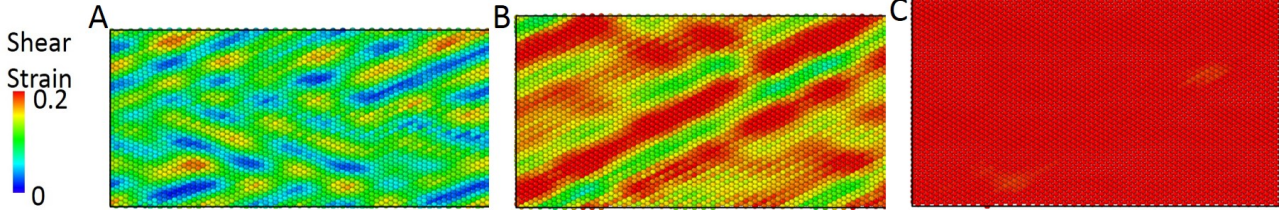


Figure 2: Phase transformation process for Si II→Si I under uniaxial unloading. (A) Heterogeneous nucleation of silicon I due to stress fluctuation. (B) Formation of band-like structure consisting of almost complete Si I and some intermediate phase, but without Si II. (C) Final stable state of Si I.

we cannot claim from this homogenous simulation result that instability point is the same as for prescribed σ . However, if starting with a band structure at larger strain, the first Piola-Kirchhoff stress increases (strain reduces) toward instability point I , heterogeneous structure is retained in the vicinity of instability point I and disappears after crossing it (Fig. 3), similar to the case with controlled Cauchy stress. Thus, multiple solutions (including homogenous and various heterogeneous) are observed after maximum in the Cauchy stress I , which confirms our analytical result that instability stress is independent of the type of prescribed stress. We believe that if we would solve the problem for a much longer time between maxima in σ and \mathbf{P} , then proper fluctuation will lead to heterogeneous solution as well.

For strain-controlled loading, the equilibrium stress-strain curve is determined in Fig. 3b, which is the same for direct and reverse PTs. Stress-strain curves for direct and reverse PTs under controlled \mathbf{P} and σ differ slightly but are still very close to each other and curves for strain-controlled loading, despite the finite loading rate. Again, while initial homogenous structure persisted until $E = 0.2927$, if we instead started with larger strain and a two-phase microstructure and reduced the strain, the heterogeneous microstructure is retained until instability point I . Since multiple solutions exist for $E > 0.2293$, $E = 0.2293$ is the instability point for prescribed strain as well.

C. Confirmation of lattice instability criterion

The main result is that *instability stresses for both direct and reverse PTs for the broad variation of all three stresses are described within high accuracy by the criterion (12)*, see Figs. 4-5. Thus, it is sufficient to find just two material parameters for two different stress states in order to describe instability at any other stress states. For direct PT, these parameters

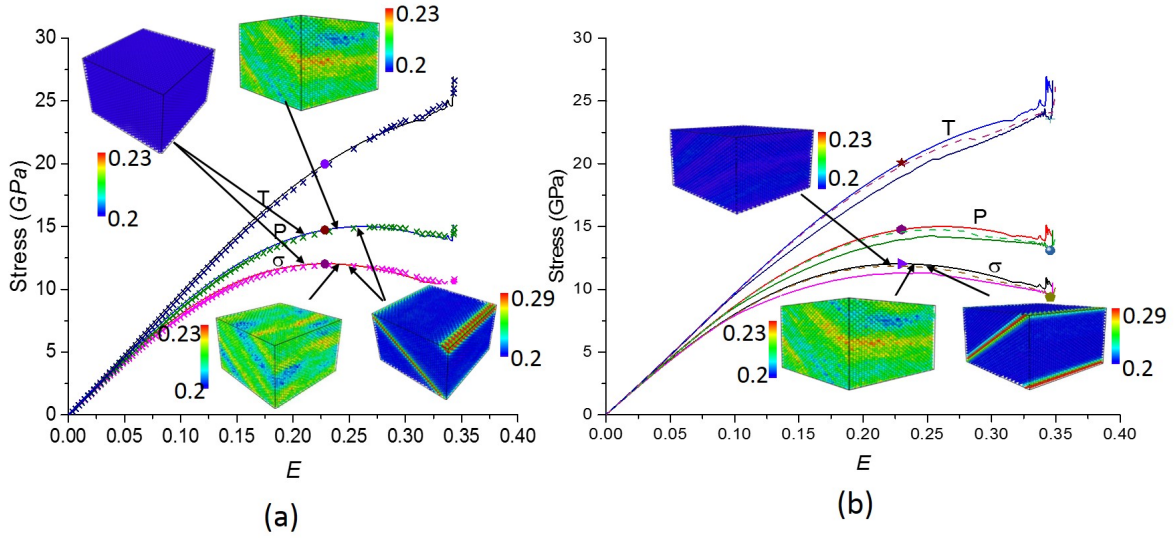


Figure 3: Stress - Lagrangian strain \mathbf{E} curves for uniaxial compression ($\sigma_1 = \sigma_2 = 0$) for the Cauchy $\boldsymbol{\sigma}$, the first Piola-Kirchhoff \mathbf{P} , and the second Piola-Kirchhoff stress \mathbf{T} for direct and reverse PTs Si I \leftrightarrow Si II. Dots mark instability points, which correspond to stresses above (or below for reverse PT) which crystal cannot be at equilibrium at prescribed $\boldsymbol{\sigma}$ or multiple (homogeneous and heterogeneous) microstructures exist. After loss of stability, the microstructure initially evolves homogeneously, then heterogeneously with stochastic fluctuations, then with bands consisting of some intermediate phases and, at larger strains, bands with fully formed Si II. Heterogeneous microstructures in Fig. 3 are obtained from two phase band structures at larger strains by returning toward instability point I. (a) Results obtained for prescribed $\boldsymbol{\sigma}$ (lines) and \mathbf{P} (symbols) are not distinguishable. Microstructures near $\boldsymbol{\sigma}$ and \mathbf{P} curves are obtained under corresponding prescribed stresses $\boldsymbol{\sigma}$ and \mathbf{P} , respectively. (b) Stress - strain curves for strain controlled loading (dashed lines), which are the same for direct and reverse PTs, in comparison with curves under controlled stresses for direct (upper lines) and reverse (lower lines) PTs.

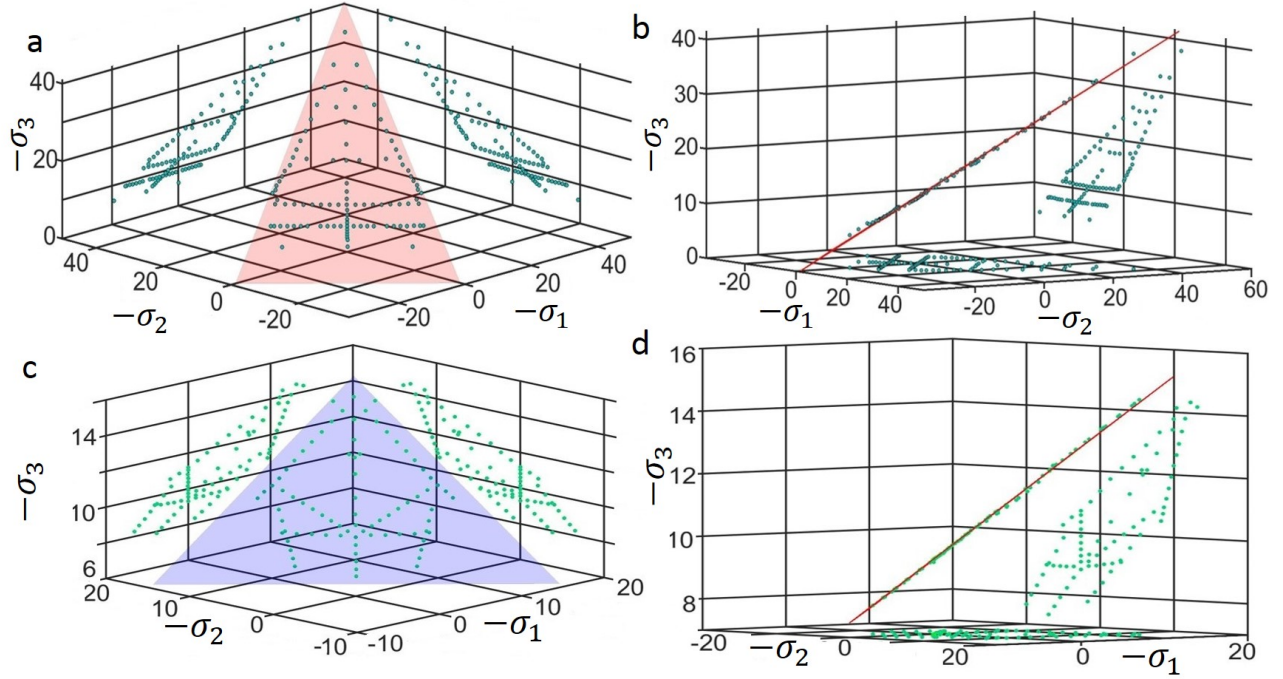


Figure 4: Conformation of lattice instability criterion (12). (A) Plane in stress space corresponding to the instability criterion (12) for direct Si I \rightarrow Si II PT and instability points from MD simulations, along with projection of each point on $\sigma_i - \sigma_j$ planes. (B) The same plot but rotated until theoretical plane (12) is visible as a line, to demonstrate how close all simulation points are to the theoretical plane. (C) and (D) are the same but for reverse Si II \rightarrow Si I PT.

are $A(\theta)/a_1 = 4.27\text{GPa}$ and $a_2/a_1 = 0.76$, for the reverse PT $A(\theta)/a_1 = -7.83\text{GPa}$ and $a_2/a_1 = 1.03$; all are determined by the best fit to MD data in Fig. 4. In particular, for $\sigma_1 = \sigma_2$, both instability lines are combined in Fig. 5A. Due to different slopes, stress hysteresis (i.e., difference between the instability stress for the direct and reverse PTs) reduces to zero toward intersection point. This leads to several interesting phenomena discussed in [24], in particular, to hysteresis- and dissipation-free homogeneous PTs between Si I and Si II, as well as to continuum of intermediate phases that are in indifferent thermodynamic equilibrium.

According to criterion (12), if one varies σ_2 while keeping $\sigma_1 = -\sigma_2$, critical σ_3 for instability should not change. It looks counterintuitive from traditional wisdom because such a loading changes the symmetry of a lattice in the 1 – 2 plane. However, this prediction is confirmed in Fig. 5B for both direct and reverse PTs with high accuracy.

Note that the parameter J for Si I \rightarrow Si II PT varies between 0.780 and 0.942 for our simulation results, i.e., by 20%. If the multiplier J was not introduced in front of $\check{\psi}^\theta$ in

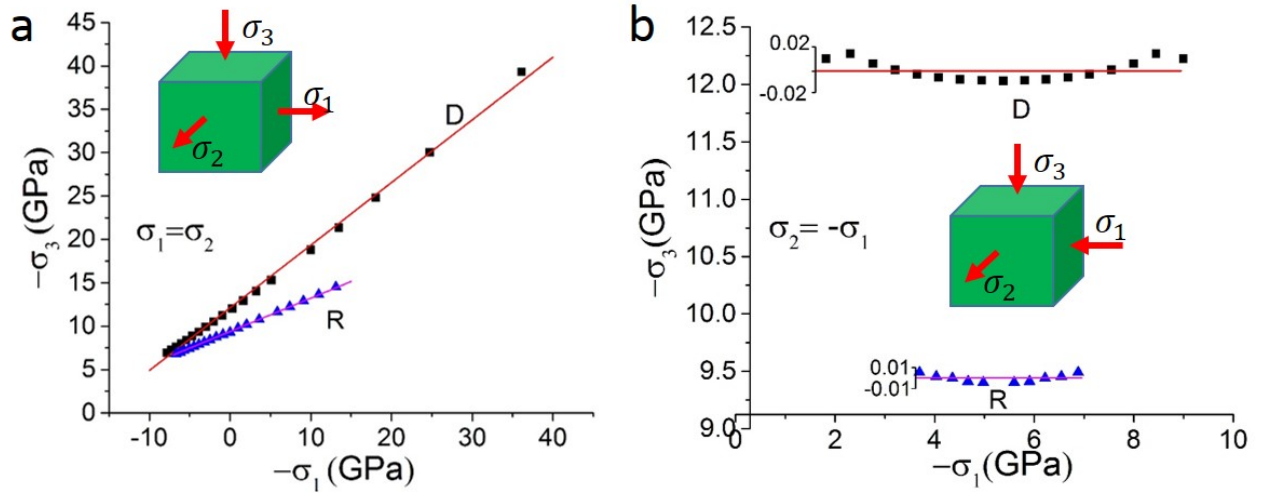


Figure 5: Relationships between stresses σ_2 and σ_3 corresponding to the lattice instability for direct (D) and reverse (R) Si I \leftrightarrow Si II PTs for (A) $\sigma_1 = \sigma_2$ and (B) $\sigma_1 = -\sigma_2$. Bars in (B) show relative error of the simulation results relatively theoretical prediction.

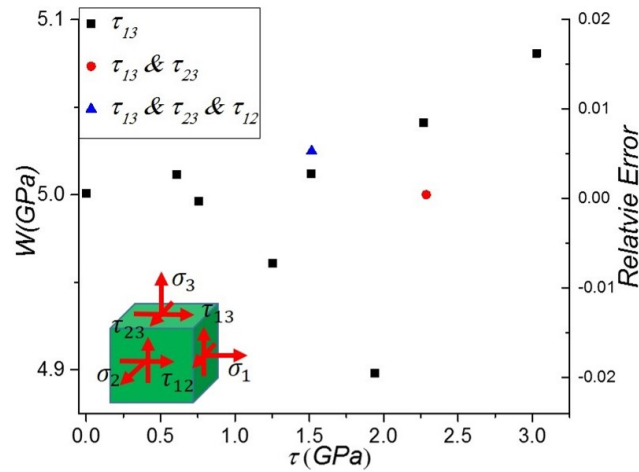


Figure 6: Modified transformation work in the instability criterion (11) versus maximum shear stress for normal stresses in the ranges $\sigma_1 = 1.50 - 2.17$, $\sigma_2 = 1.41 - 1.61$, and $-\sigma_3 = 10.38 - 10.76$ GPa.

Eq.(4) for correct description of interfacial stresses, such an error would be observed between instability criterion (2) and results of the simulation. This demonstrates nontrivial consistency in the description of completely unrelated phenomena, such as instability under a homogeneous state and stresses within a finite-width interface between parent and product phases.

Also, due to the absence of off-diagonal terms in \mathbf{U}_t , shear stresses along cubic planes should not contribute to criterion (8) in the small-strain approximation, but they change symmetry of the lattice. There is a small contribution from shear stresses due to geometric nonlinearity (see Eq.(11)). Again, MD simulations prove the validity of the instability criterion (12) for applied single, double, and three shear stresses at different planes (Fig. 6): change in the modified transformation work W does not exceed $\pm 2\%$.

D. About coincidence of the modified transformation work and the generalized Born conditions

It is intriguing that the criterion (12) also corresponds to the generalized Born condition in terms of Cauchy stress for direct PT. Explanation of this coincidence is the future challenging problem, which hopefully will lead to a new understanding of the nature of crystal instabilities. However, even now, this coincidence has three important consequences.

(a) It explains why the generalized Born condition was successful for the description of many results [2, 3, 4, 5, 11, 12], and it is not in contradiction with the criterion (12).

(b) While the choice of the stress measure in the previous instability conditions was arbitrary [2, 3] (which lead to the choice of the instability criterion without proper justification), current results clarify that it should be the Cauchy stress.

(c) The unexpected result that the generalized Born conditions are met at the plane (12) in stress space creates a strong constraint on the formulation of the nonlinear elasticity rule. This should lead to significant progress in the formulation of higher-order elastic potential, stress-strain relationships, and, consequently, Landau potential for large strains.

One of the important physical questions is: what is the order parameter, which, by definition, describes instability? There are three options:

(a) It can be related to some combination of components of the strain tensor, which results in the generalized Born instability condition. This direction was initiated in [32] and is still

broadly represented. However, since zero-moduli instability condition is not applicable at least to Si II \rightarrow Si I PT, the order parameter cannot be related to the components of the strain tensor.

(b) It can be related to some shuffles, which would result in all the equations obtained here. However, the present MD simulations of Si I to Si II transformations show that the displacements of all atoms inside the crystal cell correspond to the same \mathbf{F} which agrees with the Cauchy-Born hypothesis. That is, we cannot identify any shuffles, which are independent of \mathbf{F} .

(c) Because instability is described in terms of components of the transformation deformation gradient \mathbf{U}_t , the order parameter in this work is unambiguously and naturally related to each components of \mathbf{U}_t through interpolation functions $\varphi(a, \eta)$ (Eq.(3)), which satisfy the above formulated conditions. This is an important conclusion for the development of the Ginzburg-Landau-type theories.

Traditionally, instability criterion is evaluated for the current equilibrium state of the crystal lattice and is independent of its final state, i.e., product phase. However, instability criterion (12) includes transformation strain, i.e., it depends on the final state of the lattice. This is a seeming contradiction. Indeed, the transformation strain appears in the instability criterion because of specific interpolation function (3) chosen in our theory. However, multiplication of the components of the transformation strain in Eq.(12) by different multipliers a_1 and a_2 changes transformation strain to a different tensor, which is not related to the product phase.

CONCLUDING REMARKS

A conceptually novel approach and a specific crystal lattice instability criterion, which predicts the initiation of the first-order PTs in materials under general multiaxial loadings, are developed and validated by combining Landau-type theory and MD simulations. In contrast to the existing traditional instability criteria, the continuum approach includes an order parameter, which describes the entire dissipative transformation process. The proposed general criterion is rigorously derived utilizing the second law of thermodynamics. The criterion represents material properties and is independent of the type of the prescribed stress or strain measures. Input from MD simulations allowed us to present the instability criterion in the form of Eq.(12), which is linear in all stress components and can be calibrated by simulations at only

two different stress states. All three shear stresses do not affect instability visibly, which directly follows from our theory but sounds very counterintuitive compared to traditional approaches. The criterion is validated through hundreds of MD simulations, for Si I \leftrightarrow Si II PTs under various combinations of three normal and three shear stresses. The correspondence between criterion (12) and simulations is excellent, deviation does not exceed 2 %. Thus, it represents a predictive analytical tool, which determines how to combine six stress components to initiate various PTs. Previous approaches did not supply an analytical expression and require numerical simulations for each stress state. That is why there was no data in literature for PT criteria under more than two stresses. The obtained results also significantly advance the generalized Landau-type theory for PTs in terms of unexpected dependence of transformation strain, elastic and thermal parts of the free energy versus an order parameter.

We expect that the obtained results will stimulate similar ab initio studies and experimental measurements of lattice instabilities under multiaxial loading in order to check the validity of instability criterion (12). However, direct experimental proof is not straightforward due to the presence of defects which cause local lattice instability before external stresses reach criterion (12). We may speculate that defects can modify the parameters in criterion (8), but criterion (12) still remains linear in stress relationships; this will be checked numerically with the Ginzburg-Landau approach [33] calibrated by results obtained here. There is a confirming experimental result [34] for variant-variant transformation in Cu-Al-Ni alloy under biaxial tension. Also, similar linear stress conditions for initiation of plastic flow in metallic glasses were revealed in MD simulations in [35] which may indicate that our theoretical approach will also be applicable for this instability, as well as dislocations, twinning, and different types of PTs. Another important result of the current study is enabling the quantitative estimation of the strong effect of nonhydrostatic stresses on high pressure PTs, which is observed experimentally and utilized to drastically reduce transformation pressure [16, 36, 37].

Acknowledgments

All authors acknowledge support of NSF (CMMI-1536925) and the Extreme Science and Engineering Discovery Environment (XSEDE allocations TG-MSS170003, TG-MSS140033, and MSS170015). VIL also acknowledge support of NSF (DMR-1434613), ARO (W911NF-17-1-0225), ONR (N00014-16-1-2079), and Iowa State University (Schafer 2050 Challenge Profes-

sorship).

APPENDIX: SOME EQUATIONS AND DERIVATIONS

1. Material properties in the generalized Landau theory

We would like to enforce that for stable or metastable bulk phases $\eta = \hat{\eta}$, where $\hat{\eta} = 0$ for phase 1 and $\hat{\eta} = 1$ for phase 2. It is convenient to express any material property M (e.g., transformation strain \mathbf{U}_t , elastic moduli of i^{th} order $\mathbf{C}^i(\eta)$, $i = 2, 3, \dots$, energy, entropy, specific heat, etc.) in the form

$$M(\eta, \theta) = M_1(\theta) + (M_2(\theta) - M_0(\theta))\varphi_m(\eta), \quad (\text{A13})$$

where M_1 and M_2 are values of the property M in bulk phases 1 and 2, respectively, and $\varphi_m(\eta)$ is the corresponding interpolation function, which satisfies evident conditions

$$\varphi_m(0) = 0, \quad \varphi_m(1) = 1. \quad (\text{A14})$$

2. Thermodynamic equilibrium condition for the order parameter

However, it is not sufficient to verbally impose that $\eta = 0$ corresponds to phase 1 and $\eta = 1$ corresponds to phase 2. This should directly follow from the thermodynamic equilibrium condition for the order parameter η , which is $X = 0$. Thus, we impose the following condition:

The set of constant order parameter $\eta = \hat{\eta}$ should satisfy the thermodynamic equilibrium condition

$$X = \mathbf{P}^T \cdot \mathbf{F}_e : \frac{\partial \mathbf{U}_t(\eta)}{\partial \eta} - \frac{\partial \psi(\mathbf{E}_e, \theta, \eta)}{\partial \eta} = 0 \quad (\text{A15})$$

for any stress \mathbf{P} , temperature θ , and corresponding elastic deformation gradient \mathbf{F}_e . Otherwise, thermodynamic equilibrium values of the order parameter obtained from the condition $X = 0$ will depend on \mathbf{P} and/or θ . Substituting them in Eq.(A13) will introduce artificial temperature and stress dependence of the property M and will not allow known properties M_1 and M_2 for bulk phases 1 and 2 to be obtained.

Due to the independence of \mathbf{U}_t and ψ , Eq.(A15) splits into two equations:

$$\frac{\partial \mathbf{U}_t(\hat{\eta})}{\partial \eta} = 0; \quad \frac{\partial \psi(\mathbf{E}_e, \theta, \hat{\eta})}{\partial \eta} = 0. \quad (\text{A16})$$

Also, following from Eq.(A16), for any material property one has

$$\frac{d\varphi_m(0)}{d\eta} = \frac{d\varphi_m(1)}{d\eta} = 0. \quad (\text{A17})$$

These constraints play a crucial role in finding equations for \mathbf{U}_t and ψ as well as lattice instability criterion.

3. Criterion for the instability of the thermodynamic equilibrium under prescribed first Piola-Kirchhoff stress \mathbf{P}

Instability of the homogeneous equilibrium state under homogeneous perturbations, i.e., for material point, can only be analyzed for prescribed boundary conditions for some stress measure. We will start with prescribed nominal stress—i.e., the nonsymmetric first Piola-Kirchhoff stress \mathbf{P} .

Definition. If a spontaneous deviation of the order parameter $\Delta\eta$ from the thermodynamic equilibrium values $\hat{\eta}$ is thermodynamically admissible under prescribed boundary conditions – that is, dissipation rate $D \geq 0$ – then the thermodynamic equilibrium is unstable.

Thus, one has the following condition:

$$X(\mathbf{P}, \mathbf{F}_e + \Delta\mathbf{F}_e, \hat{\eta} + \Delta\eta) \dot{\eta} \geq 0 \quad \rightarrow \quad \text{equilibrium of phase } \hat{\eta} \text{ is unstable}, \quad (\text{A18})$$

for stress $\mathbf{P} = \mathbf{const}$ and the elastic deformation gradient \mathbf{F}_e that varies due to spontaneous variation in η . Developing the Taylor series of X around equilibrium values $\hat{\eta}$ while taking into account that $X(\mathbf{P}, \mathbf{F}_e, \hat{\eta}) = 0$, one obtains from Eq. (A18):

$$\left. \frac{\partial X(\mathbf{P}, \mathbf{F}_e, \hat{\eta})}{\partial \eta} \right|_{\mathbf{P}} \dot{\eta}^2 \geq 0 \quad \rightarrow \quad \left. \frac{\partial X(\mathbf{P}, \mathbf{F}_e, \hat{\eta})}{\partial \eta} \right|_{\mathbf{P}} \geq 0. \quad (\text{A19})$$

Let us find an explicit expression for $\left. \frac{\partial X}{\partial \eta} \right|_{\mathbf{P}}$ by direct differentiating the expression for X from Eq. (A15):

$$\left. \frac{\partial X}{\partial \eta} \right|_{\mathbf{P}} = \mathbf{P}^T \cdot \frac{\partial \mathbf{F}_e}{\partial \eta} : \frac{\partial \mathbf{U}_t}{\partial \eta} + \mathbf{P}^T \cdot \mathbf{F}_e : \frac{\partial^2 \mathbf{U}_t}{\partial \eta^2} - \left. \frac{\partial^2 \psi(\mathbf{E}_e, \hat{\eta})}{\partial \eta^2} \right|_{\mathbf{F}_e} - \frac{\partial^2 \psi(\mathbf{E}_e, \hat{\eta})}{\partial \eta \partial \mathbf{F}_e} : \left. \frac{\partial \mathbf{F}_e^T}{\partial \eta} \right|_{\mathbf{P}} \quad (\text{A20})$$

According to the elasticity rule,

$$\mathbf{P} \cdot \mathbf{U}_t = \frac{\partial \psi}{\partial \mathbf{F}_e} \quad \rightarrow \quad \mathbf{P} = \mathbf{f}(\mathbf{F}_e, \mathbf{U}_t, \mathbf{C}^i(\eta)), \quad (\text{A21})$$

where \mathbf{f} is some function. Differentiating Eq. (A21) one has

$$\frac{\partial \mathbf{P}}{\partial \eta} = 0 = \frac{\partial \mathbf{f}}{\partial \mathbf{F}_e^T} \cdot \frac{\partial \mathbf{F}_e(\hat{\eta})}{\partial \eta} \Bigg|_{\mathbf{P}} + \frac{\partial \mathbf{f}}{\partial \mathbf{U}_t} \cdot \frac{\partial \mathbf{U}_t(\hat{\eta})}{\partial \eta} + \frac{\partial \mathbf{f}}{\partial (\mathbf{C}^i)^T} \cdot \frac{\partial \mathbf{C}^i(\hat{\eta})}{\partial \eta}, \quad (\text{A22})$$

where number of double contractions and transposition rules correspond to the rank of \mathbf{C}^i . The second term in Eq. (A22) and the first term Eq. (A20) disappear, since, according to Eq. (A16) $\frac{\partial \mathbf{U}_t(\hat{\eta})}{\partial \eta} = 0$. The second term in Eq. (A22) is also zero because of $\frac{\partial \mathbf{C}^i(\hat{\eta})}{\partial \eta} = 0$. Then Eq. (A22) represents a system of nine homogeneous linear equations with respect to $\frac{\partial \mathbf{F}_e(\hat{\eta})}{\partial \eta}$. Since in general $\det \left(\frac{\partial \mathbf{f}}{\partial \mathbf{F}_e^T} \right) \neq 0$ (excluding some special stress states), this system has only the solution

$$\frac{\partial \mathbf{F}_e(\hat{\eta})}{\partial \eta} \Bigg|_{\mathbf{P}} = 0. \quad (\text{A23})$$

Thus, the fourth term in Eq. (A20) also disappears and Eq. (A20) simplifies to our general instability criterion Eq. (2).

4. Instability of the thermodynamic equilibrium for an arbitrary prescribed stress

We assume that some stress measure $\tilde{\mathbf{T}}$ is kept constant instead of the first Piola-Kirchhoff stress measure \mathbf{P} . Let it be connected to \mathbf{P} through via some function $\mathbf{P} = \phi(\tilde{\mathbf{T}}, \mathbf{F}) = \phi_1(\tilde{\mathbf{T}}, \mathbf{F}_e, \mathbf{U}_t(\eta)) = \phi_2(\tilde{\mathbf{T}}, \mathbf{F}_e, \eta)$. Performing exactly the same procedure as above but at a fixed stressed $\tilde{\mathbf{T}}$, we derive instead of Eq.(A19) the following equation

$$\frac{\partial X(\tilde{\mathbf{T}}, \mathbf{F}_e, \hat{\eta})}{\partial \eta} \Bigg|_{\tilde{\mathbf{T}}} \geq 0. \quad (\text{A24})$$

Let us determine an explicit expression for $\frac{\partial X}{\partial \eta} \Big|_{\tilde{\mathbf{T}}}$ by direct differentiating the expression for X from Eq. (A15):

$$\begin{aligned} \frac{\partial X}{\partial \eta} \Bigg|_{\tilde{\mathbf{T}}} &= \frac{\partial \mathbf{P}^T}{\partial \eta} \Bigg|_{\tilde{\mathbf{T}}} \cdot \mathbf{F}_e \cdot \frac{\partial \mathbf{U}_t}{\partial \eta} + \mathbf{P}^T \cdot \frac{\partial \mathbf{F}_e}{\partial \eta} \Bigg|_{\tilde{\mathbf{T}}} \cdot \frac{\partial \mathbf{U}_t}{\partial \eta} + \mathbf{P}^T \cdot \mathbf{F}_e \cdot \frac{\partial^2 \mathbf{U}_t}{\partial \eta^2} \\ &\quad - \frac{\partial^2 \psi(\mathbf{E}_e, \hat{\eta})}{\partial \eta^2} \Bigg|_{\mathbf{E}_e} - \frac{\partial^2 \psi(\mathbf{E}_e, \hat{\eta})}{\partial \eta \partial \mathbf{F}_e} \cdot \frac{\partial \mathbf{F}_e^T}{\partial \eta} \Bigg|_{\tilde{\mathbf{T}}}. \end{aligned} \quad (\text{A25})$$

The first two terms in Eq. (A25) disappear according to Eq. (A16). We will demonstrate that the last term in Eq. (A25) is zero as well.

We will start by assuming that $\tilde{\mathbf{T}}$ is a nonsymmetric stress tensor. Then, the elasticity rule can be presented in the form $\tilde{\mathbf{T}} = \mathbf{q}(\mathbf{F}_e, \mathbf{U}_t), \mathbf{C}^i(\hat{\eta})$, with some function \mathbf{q} . Differentiating the elasticity rule with respect to η at $\tilde{\mathbf{T}} = \mathbf{const}$, we derive

$$0 = \frac{\partial \mathbf{q}}{\partial \mathbf{F}_e^T} \cdot \frac{\partial \mathbf{F}_e(\hat{\eta})}{\partial \eta} \Big|_{\tilde{\mathbf{T}}} + \frac{\partial \mathbf{q}}{\partial \mathbf{U}_t} \cdot \frac{\partial \mathbf{U}_t(\hat{\eta})}{\partial \eta} + \frac{\partial \mathbf{q}}{\partial (\mathbf{C}^i)^T} \cdot \frac{\partial \mathbf{C}^i(\hat{\eta})}{\partial \eta}. \quad (\text{A26})$$

The last two terms are equal to zero, and since in general $\det \left(\frac{\partial \mathbf{q}}{\partial \mathbf{F}_e^T} \right) \neq 0$ (excluding some special stress states for some special stress measures), a system of nine linear equations (A26) has the only solution:

$$\frac{\partial \mathbf{F}_e(\hat{\eta})}{\partial \eta} \Big|_{\tilde{\mathbf{T}}} = 0. \quad (\text{A27})$$

Thus, the last term in Eq. (A25) disappears, and we arrive at the instability criterion Eq. (2) for any prescribed stress measure.

If $\tilde{\mathbf{T}}$ is a symmetric tensor, for example, Cauchy stress $\boldsymbol{\sigma}$, then Eq. (A26) represents six equations only, with nine unknowns. To exclude arbitrariness of the rigid-body rotation, an additional kinematic constraint should be given, which can be expressed in the form of three scalar equations $\mathbf{j}(\mathbf{F}_e \cdot \mathbf{U}_t) = \mathbf{const}$. For example, one can impose in component form

$$F_{21} = \{\mathbf{F}_e \cdot \mathbf{U}_t\}_{21} = 0, \quad F_{23} = \{\mathbf{F}_e \cdot \mathbf{U}_t\}_{23} = 0, \quad F_{31} = \{\mathbf{F}_e \cdot \mathbf{U}_t\}_{31} = 0. \quad (\text{A28})$$

Differentiating the equation of kinematic constraint with respect to η obtains

$$0 = \frac{\partial \mathbf{j}}{\partial \mathbf{F}_e^T} \cdot \frac{\partial \mathbf{F}_e(\hat{\eta})}{\partial \eta} + \frac{\partial \mathbf{j}}{\partial \mathbf{U}_t} \cdot \frac{\partial \mathbf{U}_t(\hat{\eta})}{\partial \eta}. \quad (\text{A29})$$

Again, the second term is equal to zero. Since in general the determinant of the system of nine linear equations (A26) and (A29) is not equal to zero, we again obtain Eq. (A27).

Thus, again the last term in Eq. (A25) disappears, and we arrive at the instability criterion Eq. (2) for any prescribed stress measure. Independence of the instability criterion of the boundary conditions is a very unexpected result. It is a direct consequence of conditions (A16) related to the independence of the thermodynamic equilibrium value of the order parameter and consequently, the transformation strain of the stresses and temperature.

5. Evaluating the term $\frac{\partial^2(J\check{\psi}^\theta)}{\partial\eta^2}$ in the instability criterion

Evaluation of all terms in the instability criterion (2) after substitution of explicit expressions for \mathbf{U}_t (Eq. 3) and ψ (Eq. (5)) is straightforward with only one exception. It is related to the new multiplier J in the term $J\check{\psi}^\theta(\theta, \eta)$ due to interfacial stresses (see [19]), which was not considered in [18]. First we prove that according to Eqs. (A16) and (A27),

$$\frac{\partial\mathbf{F}(\hat{\eta})}{\partial\eta} = \mathbf{F}_e \cdot \frac{\partial\mathbf{U}_t(\hat{\eta})}{\partial\eta} + \frac{\partial\mathbf{F}_e(\hat{\eta})}{\partial\eta} \cdot \mathbf{U}_t(\hat{\eta}) = 0. \quad (\text{A30})$$

Then, we evaluate

$$\frac{\partial(J\check{\psi}^\theta)}{\partial\eta} = \check{\psi}^\theta \frac{\partial J}{\partial\mathbf{F}^T} : \frac{\partial\mathbf{F}}{\partial\eta} + J \frac{\partial\check{\psi}^\theta}{\partial\eta} \quad (\text{A31})$$

and

$$\frac{\partial^2(J\check{\psi}^\theta(\hat{\eta}))}{\partial\eta^2} = \check{\psi}^\theta(\hat{\eta}) \frac{\partial}{\partial\eta} \left(\frac{\partial J}{\partial\mathbf{F}^T} : \frac{\partial\mathbf{F}}{\partial\eta} \right) + 2 \frac{\partial\check{\psi}^\theta(\hat{\eta})}{\partial\eta} \frac{\partial J}{\partial\mathbf{F}^T} : \frac{\partial\mathbf{F}(\hat{\eta})}{\partial\eta} + J \frac{\partial^2\check{\psi}^\theta(\hat{\eta})}{\partial\eta^2} = J \frac{\partial^2\check{\psi}^\theta(\hat{\eta})}{\partial\eta^2}. \quad (\text{A32})$$

Indeed, the first term in Eq. (A32) disappears because $\check{\psi}^\theta(\hat{\eta}) = 0$ and the second term is zero because of Eq. (A30). Eq. (A32) was used in transferring from Eq.(2) to Eq.(6). Also note that if the instability criterion would depend on the prescribed boundary condition, then it could not be interpreted as the local phase-transformation criterion in an arbitrary material point during solution of the boundary-value problem. Indeed, each material point undergoes a sophisticated loading process, and it is impossible to define which stress is prescribed at each point.

References

- [1] M. Born, On the stability of crystal lattices. I. *Proc. Camb. Phil. Soc.* **36**, 160-172 (1940).
- [2] R. Hill, F. Milstein, Principles of stability analysis of ideal crystals. *Phys. Rev. B* **15**, 3087-3096 (1977).
- [3] F. Milstein, J. Marschall, H. Fang, Theoretical bcc \rightarrow fcc transitions in metals via bifurcations under uniaxial load. *Phys. Rev. Lett.* **74**, 2977-2980 (1995).

- [4] J. Wang, S. Yip, S.R. Phillpot, D. Wolf, Crystal instabilities at finite strain. *Phys. Rev. Lett.* **71**, 4182-4185 (1993).
- [5] P. Alippi, P.M. Marcus, M. Scheffler, Strained tetragonal states and bain paths in metals. *Phys. Rev. Lett.* **78**, 3892-3895 (1997).
- [6] J. Morris and C. Krenn, The internal stability of an elastic solid. *Phil. Mag. A* **80**, 2827-2840 (2000).
- [7] J. Li, K.J. Van Vliet, T. Zhu, S. Yip, S. Suresh, Atomistic mechanisms governing elastic limit and incipient plasticity in crystals. *Nature* **418**, 307-310 (2002).
- [8] J. Li, T. Zhu, S. Yip, K.J.V. Vliet, S. Suresh, Elastic criterion for dislocation nucleation. *Mat. Sci. Eng. A* **365**, 25-30 (2004).
- [9] M. T. Dove, Introduction to lattice dynamics. *Cambridge University Press*, (1993).
- [10] J. Clayton, Towards a nonlinear elastic representation of finite compression and instability of boron carbide ceramic. *Phil. Mag.* **92**, 2860-2893 (2012).
- [11] G. Grimvall, M.-K. Blanka, V. Ozolins, K.A. Persson, Lattice instabilities in metallic elements. *Rev. Mod. Phys.* **84**, 945-986 (2012).
- [12] J. Pokluda, M. Cerny, M. Sob, Y. Umeno, Ab initio calculations of mechanical properties: Methods and applications. *Prog. Mater. Sci.* **73**, 127-158 (2015).
- [13] R.S. Elliott, N. Triantafyllidis, J.A. Shaw, Reversible stress-induced martensitic phase transformations in a bi-atomic crystal. *J. Mech. Phys. Solids* **59**, 216-236 (2011).
- [14] K. Gaal-Nagy, M. Schmitt, P. Pavone, D. Strauch, Ab initio study of the high-pressure phase transition from the cubic-diamond to the beta-tin structure of Si. *Comp. Mater. Sci.* **22**, 49-55 (2001).
- [15] A. Planes, L. Manosa, Vibrational properties of shape memory alloys. *Solid State Phys.* **55**, 159-267 (2001).
- [16] V.D. Blank, E.I. Estrin, Phase transitions in solids under high pressure. *Boca Raton: CRC Press*, 382-423 (2014).
- [17] See Supplemental Movies [URL].
- [18] V.I. Levitas, Phase-field theory for martensitic phase transformations at large strains. *Int. J. Plasticity* **49**, 85-118 (2013).

- [19] V.I. Levitas, Phase field approach to martensitic phase transformations with large strains and interface stresses. *J. Mech. Phys. Solids* **70**, 154-189 (2014).
- [20] P. Steve, Fast parallel algorithms for short-range molecular dynamics. *J. Comput. Phys.* **117**, 1-19 (1995).
- [21] H. Balamane, Comparative study of silicon empirical interatomic potentials. *Phys. Rev. B* **46**, 2250 (1992).
- [22] K. Mizushima, Ideal crystal stability and pressure-induced phase transition in silicon. *Phys. Rev. B* **50**, 14952 (1994).
- [23] V. Domnich, D. Ge, and Yu. Gogotsi, High Pressure Surface Science and Engineering, eds. Y. Gogotsi and V. Domnich, *Institute of Physics, Bristol*, Bristol and Philadelphia, 381-442 (2004).
- [24] V.I. Levitas, H. Chen, and L. Xiong, Triaxial-Stress-Induced Homogeneous Hysteresis-Free First-Order Phase Transformations with Stable Intermediate Phases. *Phys. Rev. Lett.* **118**, 025701 (2017).
- [25] H.J. Berendsen, J. V. Pstma, van Gunsteren, W. F. DiNola, and J. R. Haak, Molecular dynamics with coupling to an external bath. *J. Chem. Phys.* **81**, 3684 (1984).
- [26] A. K. Suhrmanian, Continuum interpretation of virial stress in molecular simulations. *Int. J. Solids Struct.* **45**, 4040-6 (2008).
- [27] M. Parrinello, Polymorphic transitions in single crystals: A new molecular dynamics method. *J. Appl. Phys.* **52**, 7182-90 (1982).
- [28] R. E. Miller, E. B. Tadmor, J. S. Gibson, J. S. Bernstein, and F. Pavia, Molecular dynamics at constant Cauchy stress. *J. Chem. Phys.* **144**, 184107 (2016).
- [29] A. Stukowski, Visualization and analysis of atomistic simulation data with OVITO: the Open Visualization Tool. *Model. Simul. Mater. Sc.* **18**, 015012 (2010).
- [30] M. L. Falk, J. S. Langer, Dynamics of viscoplastic deformation in amorphous solids. *Phys. Rev. E*, **57**, 7192 (1998).

- [31] F. Shimizu, S. Ogata, J. Li, Theory of shear banding in metallic glasses and molecular dynamics calculations. *Mater. Trans.*, **48**, 2923-2927 (2007).
- [32] G.R. Barsch, J.A. Krumhansl, Twin boundaries in ferroelastic media without interface dislocations. *Phys. Rev. Lett.* **53**, 1069-1072 (1984).
- [33] V.I. Levitas, M. Javanbakht, Phase transformations in nanograin materials under high pressure and plastic shear: nanoscale mechanisms. *Nanoscale* **6**, 162-166 (2014).
- [34] R. Abeyaratne, C. Chu, R.D. James, Kinetics of materials with wiggly energies: theory and application to the evolution of twinning microstructures in a Cu-Al-Ni shape memory alloy. *Philos. Mag. A* **73**, 457-497 (1996).
- [35] C.A. Schuh, A.C. Lund, Atomistic basis for the plastic yield criterion of metallic glass. *Nat. Mater.* **2**, 449-452 (2003).
- [36] V.I. Levitas, L.K. Shvedov, Low-pressure phase transformation from rhombohedral to cubic BN: Experiment and theory. *Phys. Rev. B* **65**, 104109 (2002).
- [37] C. Ji, V. I. Levitas, H. Zhu, J. Chaudhuri, A. Marathe, Y. Ma, Shear-induced phase transition of nanocrystalline hexagonal boron nitride to wurtzitic structure at room temperature and lower pressure. *P. Natl. Acad. Sci. USA* **109**, 19108-19112 (2012).